The following Communications have been judged by at least two referees to be "very important papers" and will be published online at www.angewandte.org soon:

News

Books

Highlights

Porous Materials

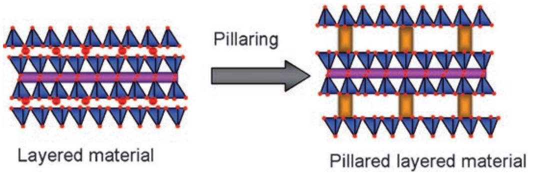

Pillaring with perfection: The construction of molecular pillars in layered materials (see scheme) while preserving the three-dimensional crystallinity enables the creation of porous structures with a narrow pore-size distribution. This method opens up a route to prepare composite materials with unusual combinations of properties.

Resolution of Alcohols

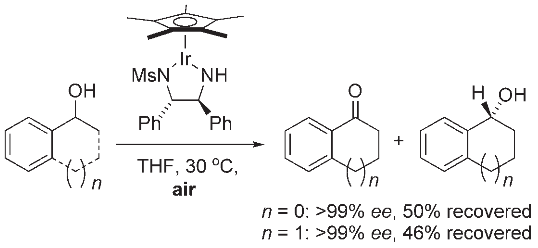

An air of excitement: Enantioselective catalysts have been developed for the kinetic resolution of racemic alcohols using aerobic oxidation. The iridium(III) complex shown (Ms = methanesulfonyl), which was developed by Ikariya et al., proved to be particularly efficient. Besides several other examples, the aspects of the mechanism are discussed.

Contents

Reviews

Ring-Closing Reactions

V. Michelet,* P. Y. Toullec,
J.-P. Genêt ———— **4268 – 4315**

Cycloisomerization of 1,*n*-Enynes: Challenging Metal-Catalyzed Rearrangements and Mechanistic Insights

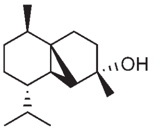

1

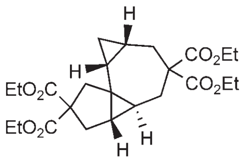

2

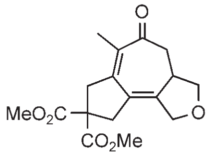

3

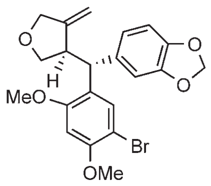

4

Rounding it up: Metal-catalyzed cycloisomerization reactions of 1,*n*-enynes are highly attractive processes as they contribute to the highly demanded search for atom economy. Besides palladium catalysts, several other metals have been identified as excellent catalysts. The molecular complexity of the synthesized products, such as **1**–**4**, can be greatly enhanced through metal-catalyzed tandem reactions.

Communications

Biosensors

L. Schröder,* L. Chavez, T. Meldrum,
M. Smith, T. J. Lowery, D. E. Wemmer,
A. Pines ———— **4316 – 4320**

Temperature-Controlled Molecular Depolarization Gates in Nuclear Magnetic Resonance

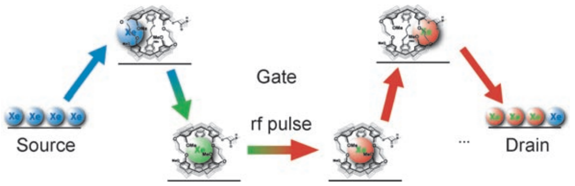

Down the drain: Cryptophane cages in combination with selective radiofrequency spin labeling can be used as molecular "transpletor" units for transferring depletion of spin polarization from a hyperpolarized source spin ensemble to a drain ensemble. The flow of nuclei through the gate is adjustable by the ambient temperature, thereby enabling controlled consumption of hyperpolarization (see scheme).

Metal–Metal Bonding

U. Flierler, M. Burzler, D. Leusser, J. Henn,
H. Ott, H. Braunschweig,
D. Stalke* ———— **4321 – 4325**

Electron-Density Investigation of Metal–Metal Bonding in the Dinuclear "Borylene" Complex $[\{Cp(CO)_2Mn\}_2(\mu\text{-}BtBu)]$

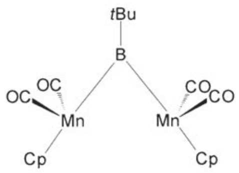

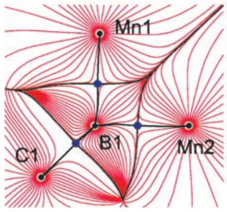

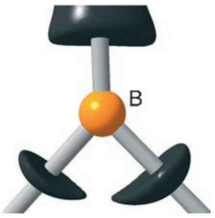

Close but not bonded are the two manganese atoms in the title borylene complex. The charge-density study demonstrates that the μ-bridging BR ligand forms valence shell charge concentrations to each metal center rather than a single one to the metal–metal midpoint as found for the isolobal C=O ligand in analogous dinuclear species.

For the USA and Canada:
ANGEWANDTE CHEMIE International Edition (ISSN 1433-7851) is published weekly by Wiley-VCH, PO Box 191161, 69451 Weinheim, Germany. Air freight and mailing in the USA by Publications Expediting Inc., 200 Meacham Ave., Elmont, NY 11003. Periodicals postage paid at Jamaica, NY 11431. US POSTMASTER: send address changes to *Angewandte Chemie*, Wiley-VCH, 111 River Street, Hoboken, NJ 07030. Annual subscription price for institutions: US$ 7225/6568 (valid for print and electronic / print or electronic delivery); for individuals who are personal members of a national chemical society prices are available on request. Postage and handling charges included. All prices are subject to local VAT/sales tax.

RNA Conformations

A. Y. Kobitski, M. Hengesbach, M. Helm, G. U. Nienhaus* ——— **4326–4330**

Sculpting an RNA Conformational Energy Landscape by a Methyl Group Modification—A Single-Molecule FRET Study

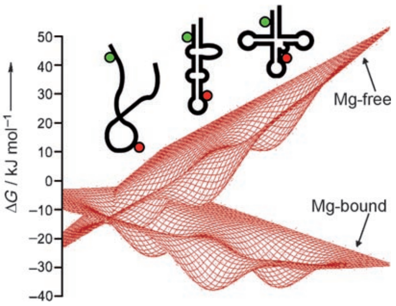

With or without Me: The effect of a single methyl group on the free energies of functional and nonfunctional conformations of human mitochondrial lysine transfer RNA (tRNA^{Lys}) has been studied. The stabilization of the three distinct conformations by Mg^{2+} ion binding and free energy changes resulting from methylation were characterized and revealed a preference for the functionally relevant cloverleaf-shaped tRNA form (see picture).

Enzyme Inhibitors

R. Löser, M. Frizler, K. Schilling, M. Gütschow* ——— **4331–4334**

Azadipeptide Nitriles: Highly Potent and Proteolytically Stable Inhibitors of Papain-Like Cysteine Proteases

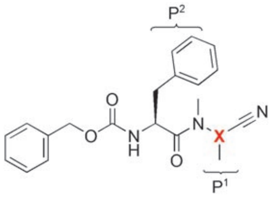

X	Conf.	K_i (Cathepsin L)
CH	S	57 μM
N	-	74 pM

Nitrogen instead of carbon: Azadipeptide nitriles resulting from CH/N exchange in the P^1 position (see picture) are hitherto unknown. To access these compounds by conversion of amino acid-derived hydrazides with cyanogen bromide both nitrogen atoms of the hydrazide must be substituted. Despite a methylated P^2-P^1 peptide bond, the azadipeptide nitriles show a strong inhibitory activity against cysteine proteases, and a high stability towards chymotryptic hydrolysis.

Natural Products (1)

A. M. Szpilman, D. M. Cereghetti, N. R. Wurtz, J. M. Manthorpe, E. M. Carreira* ——— **4335–4338**

Synthesis of 35-Deoxy Amphotericin B Methyl Ester: A Strategy for Molecular Editing

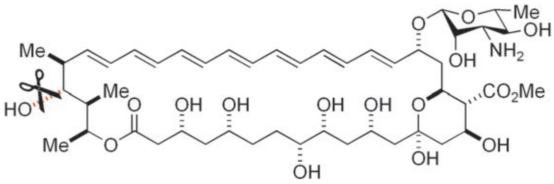

A modular strategy for the assembly of amphotericin B analogues with modifications in the macrolactone ring relies on the efficient gram-scale synthesis of all major and minor motifs of amphotericin B. Proof of concept has been achieved by the preparation of the 35-deoxy aglycone en route to the long-sought-after 35-deoxy analogue of amphotericin B.

Natural Products (2)

A. M. Szpilman, J. M. Manthorpe, E. M. Carreira* ——— **4339–4342**

Synthesis and Biological Studies of 35-Deoxy Amphotericin B Methyl Ester

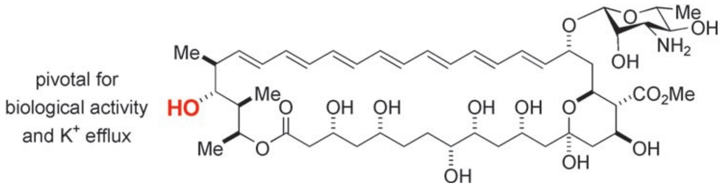

An indispensable OH group: The synthesis of 35-deoxy amphotericin B methyl ester was completed by using a novel method for the coupling of the mycosamine to the aglycone. The investigation of the antifungal activity and efflux-inducing ability of this compound provided data that underscore the relevance of the hydroxy group at C35 and supports the involvement of double-barrel ion channels.


A Journal of the Gesellschaft Deutscher Chemiker
Angewandte Chemie
International Edition
www.angewandte.org
2006–45/42
WILEY-VCH

Si, Si: The reaction of bis(lithiosilyl)mercury with $R_3Si = iPr_3Si$ with two equivalents of 1-adamantoyl chloride gave, by thermal Brook rearrangement, the first metal-substituted bis-silene. The reaction of bis(lithiosilyl)mercury having smaller $tBuMe_2Si$ substituents led to a bis(acylsilyl)mercury, which did not rearrange to the bis-silene. The effect of steric congestion on Brook rearrangement was studied computationally.

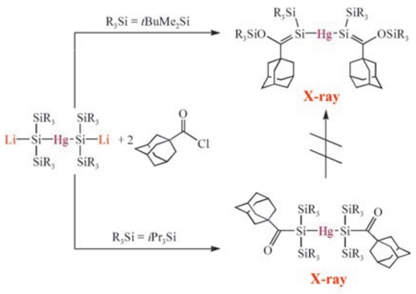

Bis-silenes

D. Bravo-Zhivotovskii,* R. Dobrovetsky, D. Nemirovsky, V. Molev, M. Bendikov, G. Molev, M. Botoshansky, Y. Apeloig* —— **4343 – 4345**

The Synthesis and Isolation of a Metal-Substituted Bis-silene

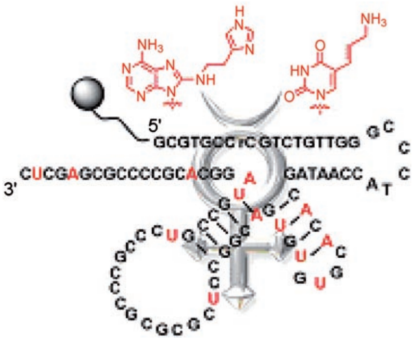

The mercury project: A self-cleaving DNAzyme that "switches on" in the presence of Hg^{2+} has been revealed by in vitro selection. The enzyme 10-13 (see picture) utilizes two modified nucleobases to confer an RNaseA-like catalytic activity that requires only Hg^{2+} and no other divalent metal cofactor. This DNAzyme is highly selective for mercuric cations.

Catalytic DNA

M. Hollenstein, C. Hipolito, C. Lam, D. Dietrich, D. M. Perrin* —— **4346 – 4350**

A Highly Selective DNAzyme Sensor for Mercuric Ions

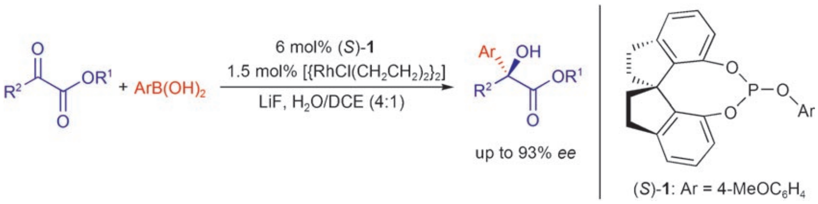

Rhodium catalysis: The first example of a catalytic asymmetric addition of arylboronic acids to α-ketoesters was realized by using a chiral Rh^I–spirophosphite ligand complex in aqueous solvent to provide tertiary α-hydroxyesters in good yields with high enantioselectivities (see scheme; DCE = 1,2-dichloroethane).

Asymmetric Catalysis

H.-F. Duan, J.-H. Xie, X.-C. Qiao, L.-X. Wang, Q.-L. Zhou* —— **4351 – 4353**

Enantioselective Rhodium-Catalyzed Addition of Arylboronic Acids to α-Ketoesters

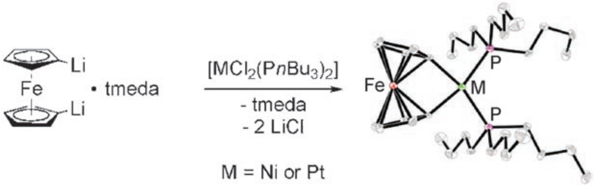

Late and unexpected: The first strained metallocenophanes with a single late transition-metal atom in the bridge have been prepared (see scheme). The nickel- and platinum-bridged complexes are the first [1]ferrocenophanes where the bridging atom has a distorted square-planar geometry, and the compounds are substantially more tilted and electron-rich than early transition-metal analogues.

Metallocenophanes

G. R. Whittell, B. M. Partridge, O. C. Presly, C. J. Adams, I. Manners* —— **4354 – 4357**

Strained Metallocenophanes with Late Transition Metals in the Bridge: Syntheses and Structures of Nickel- and Platinum-Bridged [1]Ferrocenophanes

Contents

Supported Catalysts

X. Zhang, A. Corma* ______ **4358 – 4361**

Supported Gold(III) Catalysts for Highly Efficient Three-Component Coupling Reactions

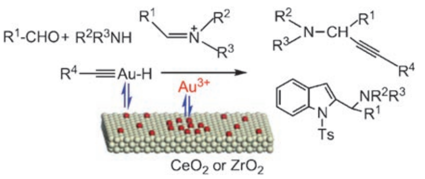

Charged gold species stabilized on nanocrystalline CeO_2 or ZrO_2 are highly active catalysts for the one-pot, three-component coupling of aldehydes, amines, and alkynes/N-protected ethynylaniline, which yields multifunctionalized propargylamines and indoles in good to excellent yields (see picture; Ts = toluene-4-sulfonyl).

Catalytic Hydrogenation

W. Baratta,* M. Ballico, G. Chelucci, K. Siega, P. Rigo ______ **4362 – 4365**

Osmium(II) CNN Pincer Complexes as Efficient Catalysts for Both Asymmetric Transfer and H_2 Hydrogenation of Ketones

Catalysis at a pinch: Osmium CNN pincer complexes [$OsCl(CNN)P_2$] (see graphic) are extremely active and productive catalysts for both the transfer and asymmetric hydrogenation of ketones (TOF ≈ 10^6 h^{-1} and TON ≈ 10^5). High enantioselectivity is achieved in the presence of only 0.005–0.002 mol% of the chiral osmium derivatives. [OsX(CNN)(dppb)] species with X = H and OR are involved in these catalytic TH and HY reactions.

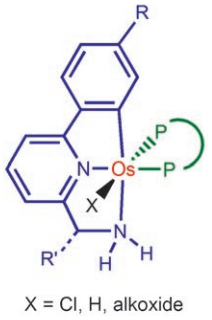

Synthetic Methods

S. Lu, Z. Xu, M. Bao,* Y. Yamamoto* ______ **4366 – 4369**

Carbocycle Synthesis through Facile and Efficient Palladium-Catalyzed Allylative De-aromatization of Naphthalene and Phenanthrene Allyl Chlorides

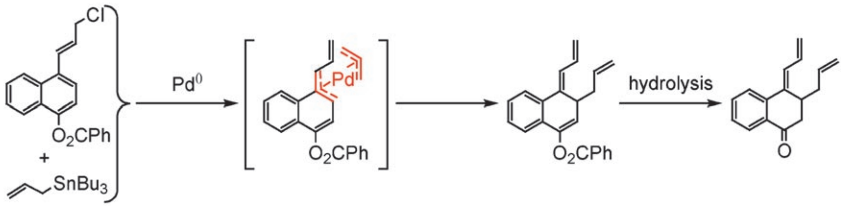

Ring of truth: The palladium-catalyzed reaction of allyltributylstannane with naphthalene or phenanthrene derivatives bearing an allyl chloride group proceeds smoothly to provide de-aromatized products with unique structures (see scheme). These products are very stable and can be used as intermediates to give fused-ring systems.

VIP

Molecular Imaging

T. Chauvin, P. Durand,* M. Bernier, H. Meudal, B.-T. Doan, F. Noury, B. Badet, J.-C. Beloeil, É. Tóth* ______ **4370 – 4372**

Detection of Enzymatic Activity by PARACEST MRI: A General Approach to Target a Large Variety of Enzymes

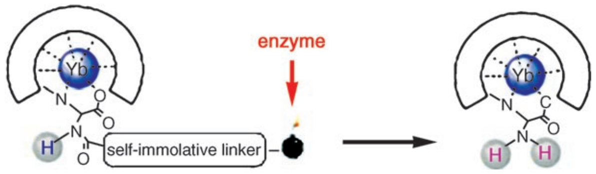

Perfect timing: A “smart” pro-PARACEST agent has been designed to detect β-galactosidase activity. Upon enzymatic attack, the self-immolative benzyloxycarbamate linker bearing the enzyme-specific substrate is cleaved and yields [Yb(dota-NH_2)]$^-$, which is endowed with a PARACEST effect. This pro-PARACEST agent is the first representative of a family of molecular imaging probes for the specific detection of a large variety of enzymatic activities using PARACEST.

Natural Product Synthesis

J. Hayashida, V. H. Rawal* ___ 4373–4376

Total Synthesis of (±)-Platencin

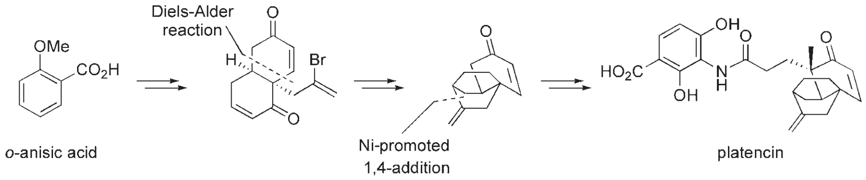

Resistant bacteria—beware! Platencin, a structurally novel broad-spectrum antibacterial agent, was the target of a total synthesis from *o*-anisic acid (see scheme). A Diels–Alder reaction with an α-substituted cyclohexenone as well as a $[Ni(cod)_2]$-promoted 1,4-addition enables the concise and stereocontrolled formation of the core. A protecting group free coupling with an aniline unit completed the synthesis. cod = 1,5-cyclooctadiene.

Natural Products

R. Tong, F. E. McDonald* ___ 4377–4379

Mimicking Biosynthesis: Total Synthesis of the Triterpene Natural Product Abudinol B from a Squalene-like Precursor

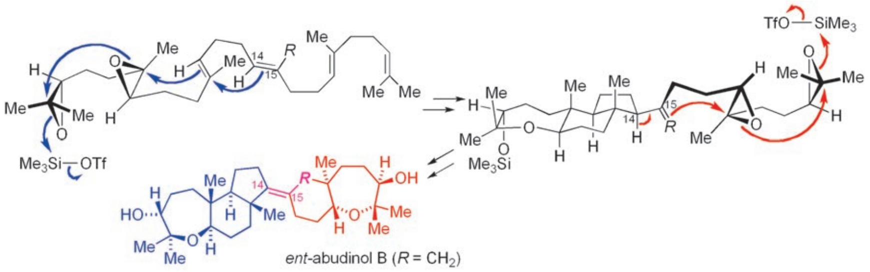

A short synthesis of the enantiomer of the title compound relies on Lewis acid promoted tandem oxa- and carbacyclizations (see scheme). This demonstration of tandem cyclizations provides experimental support for the chemical viability of a proposed biogenetic pathway.

N-Heterocyclic Ligands

S. Conejero, P. Lara, M. Paneque,
A. Petronilho, M. L. Poveda,* O. Serrano,
F. Vattier, E. Álvarez, C. Maya, V. Salazar,
E. Carmona* ___ 4380–4383

Monodentate, N-Heterocyclic Carbene-Type Coordination of 2,2′-Bipyridine and 1,10-Phenanthroline to Iridium

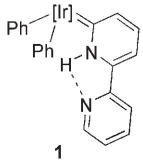

1

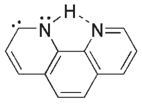

2

Unusual Carbenes: 2,2′-Bipyridine and 1,10-phenanthroline are capable of coordinating to iridium as monodentate N-heterocyclic carbene ligands stabilized by $N-H\cdots N$ bonding. This reactivity leads to complexes like **1** and their analogues with **2** as the carbene ligand. [Ir]: [hydrotris(3,5-dimethylpyrazolyl)borate]iridium.

Periodate Polyoxometalates

D.-L. Long,* Y.-F. Song, E. F. Wilson,
P. Kögerler, S.-X. Guo, A. M. Bond,
J. S. J. Hargreaves,
L. Cronin* ___ 4384–4387

Capture of Periodate in a $\{W_{18}O_{54}\}$ Cluster Cage Yielding a Catalytically Active Polyoxometalate $[H_3W_{18}O_{56}(IO_6)]^{6-}$ Embedded with High-Valent Iodine

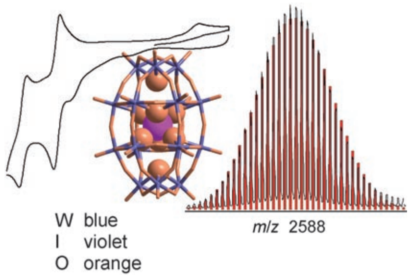

Periodate in the mix: The first crystallographically characterized tungstatoperiodate cluster of the form β^*-$[H_3W_{18}O_{56}(IO_6)]^{6-}$, with periodate embedded inside a $\{W_{18}O_{54}\}$ cluster cage, remains intact in solution, and is the first in a new class of $[H_nW_{18}O_{56}(XO_6)]^{m-}$ heteropolyoxotungstates. Mass spectrometry, and electrochemical and catalytic studies, verified by DFT calculations, reveal its unusual physical properties.

Metal Oxide Nanoassemblies

C. P. Pradeep, D.-L. Long, G. N. Newton, Y.-F. Song, L. Cronin* ______ **4388 – 4391**

Supramolecular Metal Oxides: Programmed Hierarchical Assembly of a Protein-Sized 21 kDa $[(C_{16}H_{36}N)_{19}\text{-}\{H_2NC(CH_2O)_3P_2V_3W_{15}O_{59}\}_4]^{5-}$ Polyoxometalate Assembly

Covalent grafting of “organic caps” onto Dawson metal oxide clusters controls their supramolecular self-assembly in the solid and solution phase. Formation can be controlled by changing the solvent and the hydrogen-bonding groups on the cap. A gigantic nanoassembly with a mass of ca. 21 kDa is characterized unambiguously in the solid state using single-crystal XRD, and detected in solution/gas phase by cryospray mass spectrometry as the 5^- ion.

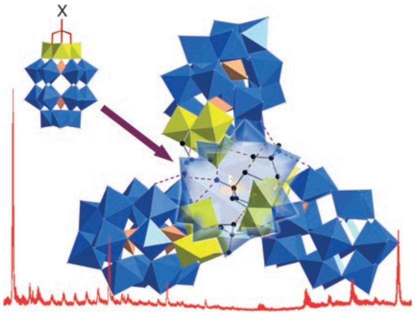

C black, O cyan, WO_4 blue, VO_4 yellow, PO_4 pink

Rotaxanes

J. Berná, S. M. Goldup, A.-L. Lee, D. A. Leigh,* M. D. Symes, G. Teobaldi, F. Zerbetto* ______ **4392 – 4396**

Cadiot–Chodkiewicz Active Template Synthesis of Rotaxanes and Switchable Molecular Shuttles with Weak Intercomponent Interactions

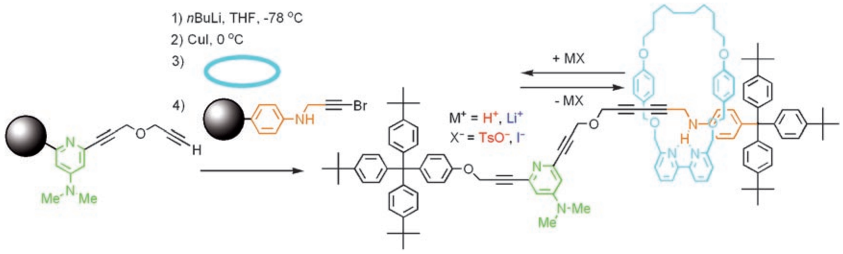

Shuttling fast and loose: Weak interaction, switchable, rotaxane-based molecular shuttles, in which the positional fidelity of the macrocycle is conferred by a single hydrogen bond in each state, are constructed through the high-yielding and selective active template heterocoupling of different functionalized alkynes using the Cadiot–Chodkiewicz reaction.

Nanostructure Assembly

H. Yang, S.-Y. Fung, M. Pritzker, P. Chen* ______ **4397 – 4400**

Mechanical-Force-Induced Nucleation and Growth of Peptide Nanofibers at Liquid/Solid Interfaces

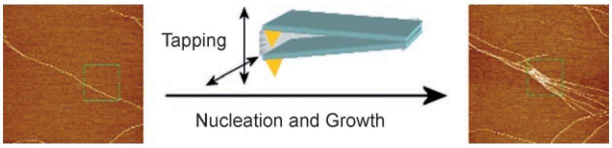

Tap to induce nanofiber growth: Mechanical force applied by a tapping AFM tip can break peptide nanofibers into active “seeds” for local growth of new nanofibers at liquid/solid interfaces (see AFM images). The combination of such an approach with certain solution conditions allows one to fabricate peptide-nanostructure-patterned surfaces.

Zeolite Structure Elucidation

Y. Li, J. Yu,* R. Xu, C. Baerlocher, L. B. McCusker ______ **4401 – 4405**

Combining Structure Modeling and Electron Microscopy to Determine Complex Zeolite Framework Structures

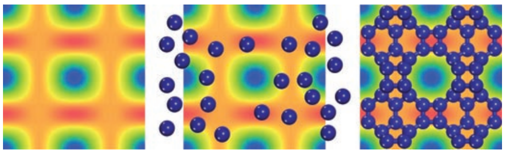

A single HRTEM image is used to build up a potential map as starting point of a computer simulation method to solve complex zeolite structures. During the simulation, atoms are generated randomly and “pushed” into regions of high potential to fit the HRTEM image (see scheme). At the end of the simulation, models with reasonable bonding geometry and good agreement with the HRTEM image are chosen as candidates for the final structure solution.

Root and branch: A two-dimensional polyimine network (see picture) is formed by condensation polymerization of trialdehydes and diamines co-adsorbed on an Au(111) surface under ultrahigh-vacuum conditions. The local bonding pattern is characterized by STM, which shows that the connectivity of the network is influenced by the kinetic parameters of the preparation procedure.

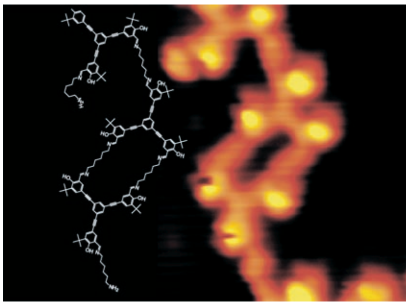

Polymer Networks

S. Weigelt, C. Busse, C. Bombis, M. M. Knudsen, K. V. Gothelf,* E. Lægsgaard, F. Besenbacher, T. R. Linderoth* **4406 – 4410**

Surface Synthesis of 2D Branched Polymer Nanostructures

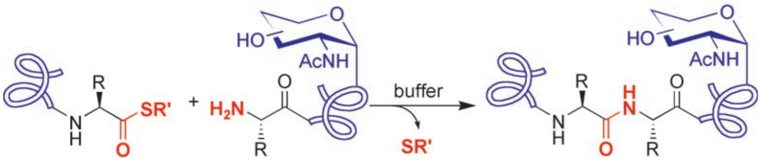

Left to their own devices in a mixed-solvent system, peptides undergo efficient aminolysis with peptide thioesters (see scheme). This ligation method, which does not require coupling reagents, auxiliaries, or an N-terminal cysteine residue, is suitable for a variety of amino acids at the ligation junction. Its effectiveness was demonstrated by the synthesis of a 6.9-kDa section of the cancer-associated MUC1 tandem repeat.

Ligation Reactions

R. J. Payne, S. Ficht, W. A. Greenberg, C.-H. Wong* **4411 – 4415**

Cysteine-Free Peptide and Glycopeptide Ligation by Direct Aminolysis

---

General patterns: A photoisomerizable nitrospiropyran monolayer associated with a gold surface enables the photolithographic patterning of the surface with nitromerocyanine domains. The selective association of Co^{2+} ions on the nitromerocyanine domains (red) allows the electrochemical generation of magnetic Co^0 nanoparticles (NPs) on these domains. The magnetic information can be electrochemically erased and restored.

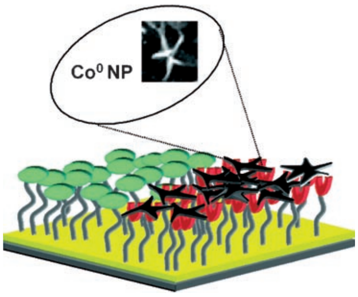

Information Storage

M. Riskin, V. Gutkin, I. Felner, I. Willner* **4416 – 4420**

Photochemical and Electrochemical Encoding of Erasable Magnetic Patterns

---

The photochemical coupling of olefin-capped (bio)molecules to surface-bound thiols can be used to control protein immobilization on length scales of centimeters to sub-micrometers (see the fluorescence microscopy image of a nanopattern after treatment with labeled streptavidin). Two enzymes immobilized on the resulting patterns retained their enzymatic activity and underwent protein–protein interactions similar to those in the solution phase.

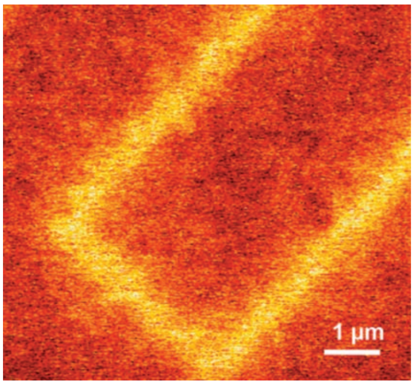

Protein Immobilization

P. Jonkheijm, D. Weinrich, M. Köhn, H. Engelkamp, P. C. M. Christianen, J. Kuhlmann, J. C. Maan, D. Nüsse, H. Schroeder, R. Wacker, R. Breinbauer, C. M. Niemeyer,* H. Waldmann* **4421 – 4424**

Photochemical Surface Patterning by the Thiol-Ene Reaction

Contents

Phosphorus Activation

P. Barbaro, M. Di Vaira, M. Peruzzini,
S. Seniori Costantini,
P. Stoppioni* ——————— **4425 – 4427**

Controlling the Activation of White Phosphorus: Formation of Phosphorous Acid and Ruthenium-Coordinated 1-Hydroxytriphosphane by Hydrolysis of Doubly Metalated P_4

Successfully tamed: When coordinated to two {CpRu(PPh$_3$)$_2$} moieties, white phosphorus (P_4) reacts selectively with a large excess of water to yield phosphorous acid (H_3PO_3) and the previously unknown 1-hydroxytriphosphane (PH(OH)PHPH$_2$), which is stabilized as a bridging ligand by coordination to the ruthenium moieties (see scheme).

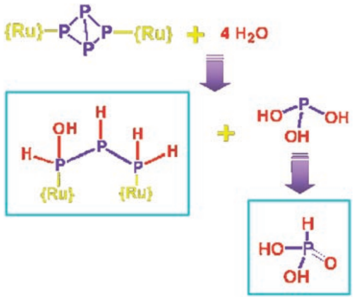

Inorganic Synthesis

Y. Liebold-Ribeiro, D. Fischer,
M. Jansen* ——————— **4428 – 4431**

Experimental Substantiation of the "Energy Landscape Concept" for Solids: Synthesis of a New Modification of LiBr

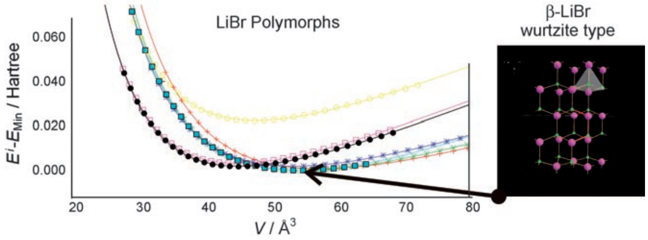

Global exploration of the energy landscape of lithium bromide led to the prediction of a new, metastable polymorph, β-LiBr (wurtzite structure type), which has now been synthesized (see *E*/*V* plot for comparison of polymorphs). Single-phase thick films of β-LiBr were obtained at −50 °C and 2.3×10^{-4} mbar using the low-temperature-deposition technique.

Antitumor Agents

S. Barluenga, C. Wang, J.-G. Fontaine,
K. Aouadi, K. Beebe, S. Tsutsumi,
L. Neckers, N. Winssinger* **4432 – 4435**

Divergent Synthesis of a Pochonin Library Targeting HSP90 and In Vivo Efficacy of an Identified Inhibitor

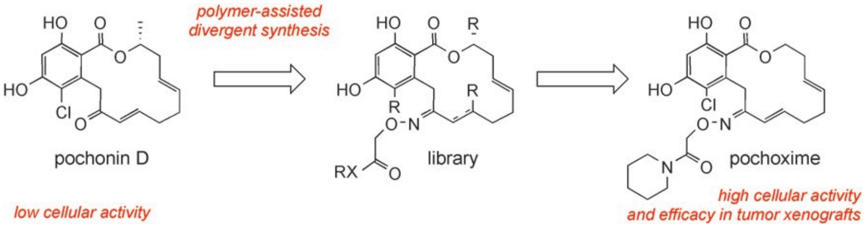

Make a clean breast of it: The generation of a library of pochonin D derivatives by a solid-phase approach has led to the discovery of pochoxime (see scheme), a potent inhibitor of the heat-shock protein 90, with over 100-fold improved incellular activity. Pochoxime was found to be effective in breast tumor xenografts, leading to a reduction in the tumor size.

Host–Guest Chemistry

S.-Y. Hsueh, K.-W. Cheng, C.-C. Lai,
S.-H. Chiu* ——————— **4436 – 4439**

Efficient Solvent-Free Syntheses of [2]- and [4]Rotaxanes

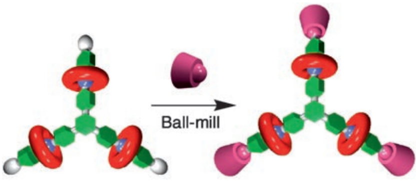

Waste not want not: A [2]rotaxane has been generated in 49 % yield through the direct grinding of solid macrocyclic, threadlike, and stoppering components. The same solid-state ball-milling reactions of solids of pseudorotaxanes and stoppers produced both [2]- and [4]rotaxanes in high yield (see picture). The approach relies on solid-state condensations and is convenient and waste-free (water is the only by-product).

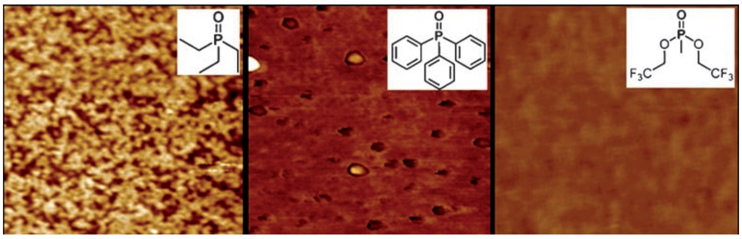

Getting a grip: H-bond formation is shown to be the main mode of interaction for monolayer formation of phosphine oxides on SiO_2 substrates (see images), with covalent reaction involved to a lesser extent. In contrast to the situation with the more widely studied polar phosphonic acids, formation of these monolayers is self-limiting. The results may have important implications for many applications based on phosphine oxide monolayers.

Supporting information is available on www.angewandte.org (see article for access details).

A video clip is available as Supporting Information on www.angewandte.org (see article for access details).

Service